STUDIES OF THE MICRO-BUNCHING INSTABILITY IN MULTI-BUNCH OPERATION AT THE ANKA STORAGE RING

M. Brosi*, E. Blomley, E. Bründermann, M. Caselle, B. Kehrer, A. Kopmann, L. Rota, M. Schedler,
P. Schönfeldt, M. Schuh, M. Schwarz, J.L. Steinmann, M. Weber and A.-S. Müller
Karlsruhe Institute of Technology, Karlsruhe, Germany

Abstract

The test facility and synchrotron light source ANKA at the Karlsruhe Institute of Technology (KIT) operates in the energy range from 0.5 to 2.5 GeV and can generate brilliant coherent synchrotron radiation (CSR) in the THz range employing a dedicated bunch length-reducing optic at 1.3 GeV beam energy. The high degree of spatial compression leads to complex longitudinal dynamics and to time evolving sub-structures in the longitudinal phase space of the electron bunches. The results of the micro-bunching instability are time-dependent fluctuations and strong bursts in the radiated THz power. To study these fluctuations in the emitted THz radiation simultaneously for each individual bunch in a multi-bunch environment, fast THz detectors are combined with KAPTURE, the dedicated KArlsruhe Pulse Taking and Ultrafast Readout Electronics system, developed at KIT. In this contribution we present measurements conducted to study possible multi-bunch effects on the characteristic bursting behavior of the micro-bunch instability.

INTRODUCTION

Due to interaction of the bunch's electric field with its own longitudinal current distribution via e.g. the resistive wall impedance or the bunch's own CSR, sub-structures form and lead to the emission of intense CSR, which again changes the longitudinal current distribution resulting in the micro-bunching instability [1]. The micro-bunching instability has been studied at several synchrotron light sources e.g. ALS [2], BESSY II [3], DIAMOND [4]. The instability occurs above a certain threshold bunch current which depends among other parameters on the bunch length and the energy spread.

At ANKA, the electron bunches can be compressed to picosecond bunch lengths by operating with a reduced momentum compaction factor α_c. In this short bunch operation mode the micro-bunching instability leads to the emission of bursts of coherent synchrotron light in the THz frequency range. The development of the temporal emission spectrum over the decreasing bunch current, see spectrogram in Fig. 1, is reproducible for the same machine parameters (like the acceleration voltage V_{RF} and α_c) [5]. With the measurement setup described in the following it is possible to measure this bursting behavior for all bunches in a multi-bunch fill individually. This allows to study possible differences in the behavior of the individual bunches caused by the presence of the surrounding bunches.
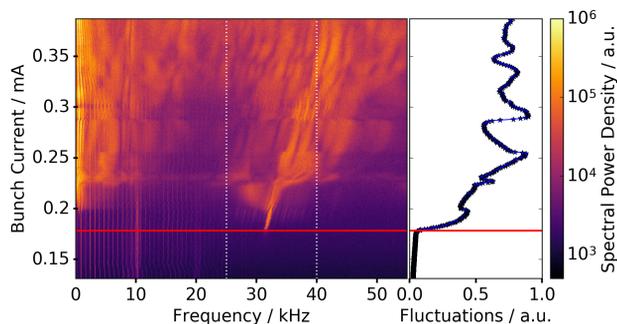
Figure 1: Temporal emission spectrum of THz intensity as function of decreasing bunch current. The red line indicates start of the fluctuations due to the micro-bunching instability. In the right panel the sum of the fluctuation power in frequency range 25 –40 kHz shows a strong increase at the threshold current.

The simplified parallel plates impedance model [6], which nicely represents the micro-bunching instability [5, 7], does not predict any interaction between the bunches due to its short-range wakefield. Yet such interaction can be facilitated by different structures present in real machines, like RF-cavities, passive cavities, scrapers and other sources of long-ranging wakefields. First indications for multi-bunch effects at ANKA were measured in 2004 [8] caused by the influence of scrapers and in 2012 based on the emitted THz power [9]. Moreover, possible effects through CSR based on whispering gallery modes were theoretically discussed and simulated [10].

In the following the threshold current, as one of the most prominent features of the instability, will be compared between the individual bunches.

MEASUREMENT PRINCIPLE

For precise studies of the instability behavior precise measurements of the CSR as well as the bunch currents are required. Firstly, fast THz detectors (in our case broadband quasi optical Schottky barrier diode detector from ACST [11] or narrow band barrier diode detector from VDI) [12] are read out using KAPTURE [13], an in-house developed fast data acquisition system based on an FPGA. This combination is used to record the peak intensity of the THz pulse emitted from each bunch at every revolution at the "Infrared2" beamline [14]. For the measurements discussed here the system was set up to record the THz pulses of all bunches at every 10th revolution over one second, repeating this measurement every 10 seconds.

The second part is to measure the bunch current of each bunch precisely over time. Therefore a combination of beam current measurement via DCCT and filling pattern measurement via time-correlated single photon counting (TCSPC) is used. The TCSPC setup is located at the visible light diagnostics port and consists of a single photon avalanche diode (id100-20 from IDquantique [15]) and a histogramming device (PicoHarp 300 from PicoQuant [16]) [17].

Systematic errors in the bunch current measurement can falsely look like systematic differences in the threshold current of the bunches (see Fig. 2). Hence, it is crucial to avoid deformations in the measured filling pattern e.g. due to dead time effects of the histogramming device. The dead time of the used PicoHarp 300 was measured to be 87 ns. The effects due to this dead time on the measured filling pattern can be estimated as described in [18]. The probability p_b that a photon is detected from bunch b at one passage is proportional to its bunch current. In a circular light source the probability $p_{b, \text{ dead time}}$ for a photon from bunch b being detected per revolution can be derived from the probability $p_{b, \text{ no dead time}}$ of a photon being detected without the dead time effects present, multiplied with the product of the probabilities that no photon was detected in the 44 previous bunches ($\hat{=}$ 87 ns):

$$p_{b, \text{ dead time}} = p_{b, \text{ no dead time}} \prod_{j=b-44}^{b-1} \left(1 - p_j\right). \quad (1)$$

The corrected number of photons ($\nu_b = N_{\text{rev}} \cdot p_b$) with the approximation that p is small is given by

$$\nu_{b, \text{ corrected}} = \frac{\nu_{b, \text{ dead time}}}{1 - \sum_{j=b-44}^{b-1} \left(\frac{\nu_j}{N_{\text{rev}}}\right)} \quad (2)$$

with the number of turns N_{rev} per acquisition time. Figure 2 shows how the effect visible vanishes when the dead time influence is corrected.

The statistical error on the bunch current measurement consists of the statistical error on the beam current measurement and the error on the filling pattern. The latter is dominated by the Poisson statistics and therefore can be calculated from the measured counts ν_b per bunch b as:

$$\frac{\sigma_{I_b}}{I_b} = \frac{1}{\sqrt{\nu_b}} \quad (3)$$

This results in a higher relative error for smaller bunch currents as the count rate is proportional to the bunch current. To reduce the measurement error a high number of counts is necessary. But as a too high count rate leads to strong systematic measurement errors due to the dead time effect, a lower count rate combined with a longer integration is favorable. With an attenuation reducing the count rate below the impact of the dead time effect, the integration time per measurement was chosen to be 30 s.

THRESHOLD DETERMINATION

The threshold of the micro-bunching instability is the bunch current above which the first fluctuations of the emitted CSR intensity occur (Fig.1). The standard deviation of
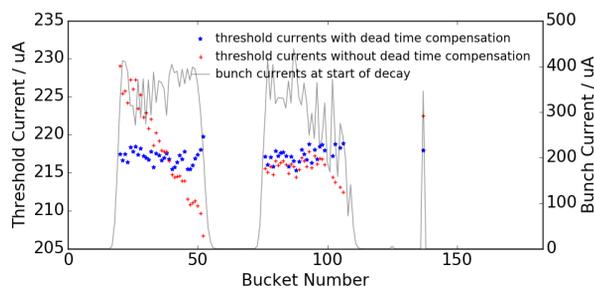

Figure 2: Threshold current per bunch as function of bunch number. Due to the dead time effect the bunch current is determined falsely, leading to differences in the threshold currents (in red). The systematic in the differences originates from the combination of the dead time duration of 87 ns (44 buckets) and the filling pattern (in grey). After the compensation of the dead time effect the systematic differences vanish and the spread decreases (in blue).

the temporal emission gives the strength of the fluctuations and is therefore an indication for the bursting threshold, as the fluctuation strength increases drastically at the threshold current [5]. Fluctuations seen below the threshold current in Fig. 1 are mainly caused by the synchrotron oscillation and 50 Hz noise and are therefore generally at lower frequencies than the first instability frequency. For the threshold determination, those lower frequency fluctuations can be omitted by using instead of the standard deviation the integrated power in fluctuations at a specific frequency range around the first instability frequency. In Figure 1 the power of the fluctuations in the frequency range from 25 –40 kHz is displayed. The threshold is strongly visible as the first increase (kink).

To determine the bunch current at the threshold for each bunch, a fit over the measured bunch current is necessary, as only every 30 s a TCSPC measurement is available. To model two contributions to the lifetime a double exponential fit was applied successfully for several measurements. However, for some machine configurations this model only seems to be applicable for some bunches while others show small but systematic differences from the fitted behavior. This could possibly lead to an artificial systematic on the distribution of the determined threshold currents. By applying the fit for all bunches only on the same fixed current range around the threshold current this effect was avoided. For these partial fits a simple exponential function (including an offset) suffices. Further investigation will show why, for some machine configurations, the same fit model does not describe the current decay for a part of the bunches in a multi-bunch environment. These differences between the bunches in the evolution of their bunch current as as function of time could hint at different beam dynamical behaviors.

RESULTS

The measured average threshold current $\mu\,(I_{\text{th}})$ of the bunches in multi-bunch fills is given in Tab. 1 for several

05 Beam Dynamics and Electromagnetic Fields

D06 Coherent and Incoherent Instabilities - Measurements and Countermeasures

Table 1: Spread of threshold current vs. statistic error on measured bunch current at threshold for different fills with different threshold currents, due to different machine settings. The (quadratic) difference between the standard deviation of the threshold currents I_{th} of the different bunches and the statistic error of the bunch current measurement at the mean threshold current $\sigma_{I_{b,th}}$ is given. To determine the bunch current at the threshold an exponential fit is used locally around the threshold current. The difference in the uncertainty on the threshold currents for the fitted data compared to the Poisson error, shows that the fit improves the quality of the bunch currents. All values are given in µA.

Fill number	6212	6258	6283	6284	6288	6292	6296
$\mu\,(I_{th})$	106.02	143.57	179.44	67.64	116.15	128.13	243.17
$\sigma_{I_{b,th},\,\text{Poisson}}$	1.98	17.26	1.79	1.20	1.38	1.45	2.10
$\sigma_{I_{b,th},\,\text{Fit}}$	0.48	4.12	0.62	0.29	0.34	0.29	0.72
$\sigma\,(I_{th})$	0.55	4.28	1.065	0.49	0.50	0.43	0.98
$\sqrt{\sigma\,(I_{th})^2 - \sigma_{I_{b,th}}^2}$ (par. exp. fit)	0.27	1.16	0.87	0.39	0.37	0.32	0.66

fills. Due to different settings of the RF-voltage and the momentum compaction factor the resulting threshold currents I_{th} differ. Figure 3 shows the fluctuation strength as a function of the bunch current for all bunches in one fill. All bunches show a similar behavior, with a small variation at the current where the signal increases strongly, indicating the instability threshold.

The statistical uncertainty $\sigma_{I_{b,th},\,\text{Poisson}}$ on the bunch current measurement at the threshold current, calculated by the Poisson statistic (Eq. 3), is around 1 to 2 µA. With the exception of fill 6258 for which the optical attenuation of the TCSPC setup was chosen stronger, leading to a lower count rate. The usage of a fit reduces the statistical fluctuations and therefore improves the uncertainty on the bunch current $\sigma_{I_{b,th},\,\text{Fit}}$ by a factor 3 or more to values below 1 µA for the most cases. The spread of the threshold currents $\sigma\,(I_{th})$ of the bunches (calculated using the partial exponential fit described above) was found to be mostly below 1 µA. Being in the same order as the uncertainty on the bunch current the resolution is not high enough to show any systematic distribution in the threshold differences.

Nevertheless, the difference between the threshold spread and the current uncertainty indicates an additional contribution to the spread in threshold currents. For the presented measurements an upper limit for the influence of multi-bunch effects on the threshold of the longitudinal micro-bunching instability can be given with approx. 0.5 µA.

SUMMARY

The threshold current of the micro-bunching instability could be an indication for multi-bunch effects as it is sensitive to changes of the longitudinal properties of a bunch, such as the effective acceleration voltage or changes in the longitudinal phase-space form due to impedances and wake fields. Fast THz detectors combined with KAPTURE allow the necessary measurement of the THz pulse of each bunch at every turn in multi-bunch fills. Using TCSPC to measure the filling pattern provides a bunch current measurement with an uncertainty of less than 1 µA. The spread between the threshold currents of the different bunches in a fill was measured to be around 1 µA indicating a possible
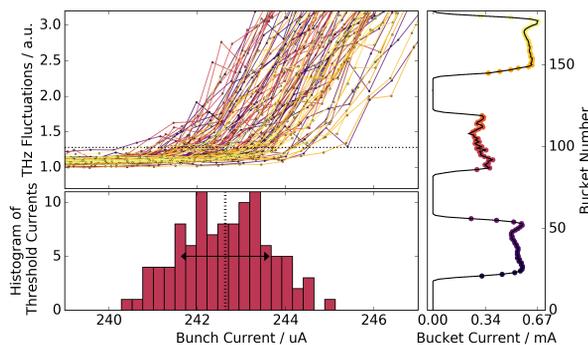

Figure 3: THz fluctuations as function of bunch current for all bunches in a multi-bunch fill. The vertical (doted) line in the histogram of the threshold currents of each bunch (lower panel) indicates the average of the threshold currents $\mu\,(I_{th})$ while the horizontal arrows indicate the spread (standard deviation) of threshold currents $\sigma\,(I_{th})$. The filling pattern at the start of the decay is indicated in the right plot.

remaining effect of 0.5 µA. In further studies the possible effects could be enlarged by introducing additional sources of long-ranging wakefields in the vacuum chamber.

ACKNOWLEDGMENT

REFERENCES

[1] G. Stupakov and S. Heifets, "Beam instability and microbunching due to coherent synchrotron radiation", Phys. Rev. STAB, 2002, Vol. 5, Nr. 5, DOI:10.1103/PhysRevSTAB.5.054402.

05 Beam Dynamics and Electromagnetic Fields

D06 Coherent and Incoherent Instabilities - Measurements and Countermeasures

[2] J. M. Byrd et al., "Observation of broadband self-amplified spontaneous coherent terahertz synchrotron radiation in a storage ring", Phys. Rev. Lett., vol. 89, iss. 22, p. 224801, 25 November 2002.

[3] P. Kuske, "Investigation of the temporal structure of CSR-bursts at BESSY II", Proc. of PAC'09, paper FR5RFP053.

[4] R. Bartolini, P.Karataev, and G. Rehm, "Observation of longitudinal microbunching instabilities in the Diamond storage ring", Proc. of PAC'09, paper FR5RFP074.

[5] M. Brosi et al., "Fast mapping of terahertz bursting thresholds and characteristics at synchrotron light sources", Phys. Rev. Accel. Beams, vol. 19, p. 110701.

[6] M. Venturini, R. Warnock, "Bursts of coherent synchrotron radiation in electron storage rings: a dynamical model", Phys. Rev. Lett., vol. 89, p. 224802, 2002.

[7] P. Schönfeldt et al., "Parallelized Vlasov-Fokker-Planck solver for desktop personal computers", Phys. Rev. Accel. Beams, vol. 20, p. 030704.

[8] A.-S. Müller et al., "Investigation of scraper induced wakefields at ANKA", Proc. of EPAC'04, paper WEPLT069.

[9] A.S. Müller et al., "Experimental aspects of CSR in the ANKA storage ring", in ICFA Beam Dynamics Newsletter No. 57, 2012, pp. 154–165.

[10] R. Warnock, J. Bergstrom, M. Klein, "Inter-bunch communication through CSR in whispering gallery modes", Proc. of NA-PAC'13, paper MOPBA19.

[11] Zero-Bias Schottky Diodes: `http://www.acst.de/`

[12] Virginia Diodes, Inc.: `http://vadiodes.com/`

[13] M. Caselle et al., "A picosecond sampling electronic 'KAPTURE' for terahertz synchrotron radiation", Proc. of IBIC'14, paper MOCZB1.

[14] Y.-L. Mathis et al., "Terahertz radiation at ANKA, the new synchrotron light source in Karlsruhe", J. Biol. Phys., vol. 29, p. 313–318, 2003.

[15] idQuantique: `http://idquantique.com`

[16] PicoQuant: `http://picoquant.com`

[17] B. Kehrer et al., "Visible light diagnostics at the ANKA storage ring", Proc. of IPAC'15, paper MOPHA037.

[18] M. Patting et al., "Dead-time effects in TCSPC data analysis", in Intl. Congress on Optics and Optoelectronics, p. 658307, 2007.